1   **Rhes, a Striatal Enriched Protein, Regulates Post-Translational Small-Ubiquitin-**

2   **like-Modifier (SUMO) Modification of Nuclear Proteins and Alters Gene**

3   **Expression**

4

5   Oscar Rivera[1*], Manish Sharma[1*] Neelam Shahani[1], Uri Nimrod Ramírez-Jarquín[1], Gogce

6   Crynen[2], Pabalu Karunadharma[3], Francis McManus[4], Thibault Pierre[4,5,], Srinivasa

7   Subramaniam[1#]

8

9   [1]Department of Neuroscience, The Scripps Research Institute, Florida, USA, 33458

10   [2]Center for Computational Biology and Bioinformatics, The Scripps Research Institute

11   Jupiter, FL. 33458, USA.

12   [3]The Scripps Research Institute, Genomic Core, Jupiter, FL 33458, USA

13   [4]Institute for Research in Immunology and Cancer, Université de Montréal,

14   Montréal, H3T 1J4, Canada

15   [5]Department of Chemistry, Université de Montréal, Montréal, Québec, Canada

16   *Contributed equally

17   #Correspondence: ssubrama@scripps.edu

18

19

20

21

22

23

24

25

26

27

28

29

30

31

32

33

34

35

36

ABSTRACT

Rhes (Ras homolog enriched in the striatum) is a multifunctional protein that orchestrates striatal toxicity, motor behaviors and abnormal movements associated with dopaminergic signaling, Huntington disease and Parkinson disease signaling in the striatum. Rhes engineers membranous tunneling nanotube-like structures and promotes intercellular protein and cargoes transport. Recent study revealed Rhes also regulates mitophagy via the Nix receptor. Despite these studies, the mechanisms through which Rhes mediates these diverse functions remains unclear. Rhes belongs to a small GTPase family member and consists of a unique C-terminal Small Ubiquitin-like Modifier (SUMO) E3-like domain that promotes the post-translational modification (PTM) of proteins with SUMO (SUMOylation) by promoting "cross-SUMOylation" of SUMO enzymes SUMO E1 (Aos1/Uba2) and SUMO E2 ligase (Ubc-9). However, the identity of the SUMO substrates of Rhes remains largely unknown. By combining high throughput interactome and SUMO proteomics we report that Rhes regulates the SUMOylation of nuclear proteins that are involved in the regulation of gene transcription. While Rhes has increased the SUMOylation of histone deacetylase 1 (HDAC1) and histone 2B, it had decreased the SUMOylation of heterogeneous nuclear ribonucleoprotein M (HNRNPM), protein polybromo-1 (PBRM1) and E3 SUMO-protein ligase (PIASy). We also found that Rhes itself is SUMOylated at 5 different lysine residues (K32, K110, K114, K120, K124 and K245). Furthermore, we found that Rhes regulates the expression of genes involved in cellular morphogenesis and differentiation in the striatum, in a SUMO-dependent manner. Our findings thus provide a previously undescribed role for Rhes in regulating SUMOylation of nuclear targets and in orchestrating striatal gene expression via the SUMOylation.

59

KEY WORDS

Medium spiny neurons, SUMO E3-ligase, Gene regulation, Brain, Differentiation, Morphology, Signaling, Perinuclear membrane.

63

64

65

66

67

68

2

69

70

71 **INTRODUCTION**

72   Rhes (Ras homolog enriched in the striatum) mRNA is highly expressed in the dopamine
73 D1 receptor (D1R)- or D2R-expressing medium spiny neurons (MSNs) and cholinergic
74 interneurons in the striatum; it is also expressed to some extent in other brain regions such as
75 cortex and hippocampus [1-3]. Rhes is induced by thyroid hormones and can inhibit the
76 cAMP/PKA pathway and N-type Ca^{2+} channels (Cav 2.2) [4-7]. We have found several new roles
77 for Rhes in the striatum. Rhes can directly bind to, and activate, mTOR in a GTP-dependent
78 manner, promoting L-DOPA-induced dyskinesia (LID) in a pre-clinical model of Parkinson's
79 disease [8]. Rhes also inhibits striatal motor activity through a 'Rhesactome"—a protein network
80 in the striatum—via its guanine nucleotide exchange factor (GEF), RasGRP1 [9], which we
81 recently found also promotes LID [10]. Rhes affects autophagy via Beclin1, independent of
82 mTOR signaling [11]. We also demonstrated a critical role for Rhes in Huntington disease (HD).
83 We found Rhes interacts with mHTT, the genetic risk factor of HD, and makes it more soluble
84 by virtue of its SUMOylation [9, 12]. Thus, Rhes and mHTT interaction increases cellular
85 toxicity, a finding which is consistent with independent studies [12-19]. One report indicates
86 that Rhes overexpression can be protective in HD [20], and so Rhes was tagged on its C-
87 terminal end in this study to promote its mislocalization to the nucleus [12]. Rhes also plays a
88 critical role in mutant tau-mediated pathology [21]. In addition, a rare, highly conserved de
89 novo mutation (R57H) in Rhes was detected in twins diagnosed on the autistic spectrum [22].

90   Recently, tubular or tunneling nanotubes (TNTs), the fragile and inconspicuous
91 membranous structures ranging from 50-200 nm diameter in size and 5-125 μm in length
92 connecting two cells, have been reported in diverse cell types [23-39]. We have discovered that
93 Rhes promotes TNT-like membranous protrusion called "Rhes tunnel" in multiple cell types,
94 including primary striatal neurons [40]. Using mutagenesis, we found that the membrane
95 binding site of Rhes (C263) is critical for Rhes tunnels. Mutagenesis also demonstrated a
96 distinct role for the GTPase domain (1-171aa) and SUMO E3 ligase domain of Rhes (171-266aa)
97 [40]. While the GTPase domain is defective in producing TNT-like protrusions, the SUMO E3
98 ligase domain induces TNTs, but shows diminished potency of cell-to-cell transport [40]. This
99 data indicates a distinct role for Rhes domain, while SUMO E3 ligase domain promote Rhes
100 tunnel, the GTPase domain is necessary for entering into the acceptor cell via Rhes tunnel.
101 Given that Rhes is the first brain-enriched protein shown to promote TNT-like protrusions, a

3

102 further investigation into its mechanisms and roles would improve our understanding of TNT-
103 like communications in brain.

104 Rhes is capable of executing more than one function, at molecular, cellular, and
105 organismal levels. Multifunctional proteins like Rhes are not rare in biology. For example,
106 through network topological information with protein annotations, it was estimated that around
107 430 of human proteins can be classed as extreme multifunctional proteins [41], including p53
108 and Cyt C [42, 43]. Despite its multiple functions and molecular complexity, fundamental
109 knowledge about the mechanisms by which Rhes works or how those mechanisms selectively
110 impair distinct striatal disorders remains partial. We reported that Rhes physiologically
111 regulates SUMO modification in vivo and mechanistically Rhes promotes the "cross-
112 SUMOylation" of E1 (Aos1) and E2 (Ubc9) enzymes [44]. However, the identity of SUMO
113 substrates of Rhes remains largely unknown. Using biochemical, proteomics and RNA seq tools,
114 we investigated the SUMO substrates of Rhes and its putative role in the striatal gene
115 expression.

116

117 **RESULTS**
118 **Rhes interacts with SUMOylated proteins and enhances SUMOylation in cultured**
119 **cells**
120 Like ubiquitin, SUMO (3 paralogues in vertebrates: SUMO1, SUMO2, and SUMO3) is a
121 conserved ~10.5kDa protein modification that is covalently attached to lysine residues
122 on multiple substrate proteins in a dynamic and reversible manner [45]. To identify
123 SUMO substrates of Rhes, we used mSUMO3 construct in combination with a large scale
124 unbiased proteomics approach for SUMOylation site identification. mSUMO3 has a mutation in
125 the C-terminal that can be cleaved by trypsin resulting in a C-terminus penta-peptide, which is
126 compatible for mass-spectrometry (MS) detection [46, 47]. We employed mSUMO3 in this study
127 because its transient expression produced more abundant protein that may aid in SUMO
128 substrate detection in HEK293 cells, compared to mSUMO1 or mSUMO2 (Fig. 1A). First, we
129 hypothesized that the SUMO proteins that binds to Rhes are the potential SUMO targets of
130 Rhes. To examine this hypothesis, we co-expressed GST-Rhes or GST (control) with His-tagged
131 mSUMO3 in HEK293 cells and affinity purified Rhes using GST-glutathione-affinity column.
132 We found GST-Rhes readily bound to proteins that are modified by mSUMO3 (Fig. 1B). The
133 GST-Rhes affinity purified samples were subjected to MS analysis to identify and quantify the
134 interacting partners. We found several proteins that are readily bound to Rhes, including RAC1,

135   TSC2, VDAC1, PLEC, DDX3X and mTOR, previously identified interactors of Rhes (Fig. 1C, Data
136   file S1)[8, 9].

137   Attempts at identifying SUMOylated interacting partners from the GST pulldown were
138   futile. Although we found targets such as RPL3 (K399), histone H4 (K6, K9, and K13) and
139   RANGAP1 (K524) found SUMOylated, the log10 transformed p value for any of the targets did
140   not reach below 0.05 (Fig. 1D) (Data file S2). We reasoned that the SUMOylated proteins that
141   are bound to Rhes are either very few or below the threshold needed for the detection by MS.
142   Moreover, GST pulldown experiments are conducted under native conditions, under which the
143   SUMO specific proteases (SENPs) are highly active and could deconjugate the SUMO moiety
144   from the target proteins[48]. Therefore, we resorted to a denaturing purification protocol to
145   enrich SUMOylated proteins. We co-expressed myc-Rhes or myc (control) with His-tagged
146   mSUMO3 in HEK293 cells and lysed the cells in guanidine-hydrochloride/urea denaturing
147   buffer, followed by purification in Ni-NTA column. We found that the myc-Rhes significantly
148   enhanced the overall SUMOylation of proteins (Fig. 1E, F) and Rhes was itself SUMOylated (S*
149   Rhes, Fig. 1E), consistent with our previous report [12].

150   Together these results indicate a) Rhes interacts with multiple proteins, and b) Rhes is
151   SUMOylated, and c) Rhes enhances the SUMOylation of several targets.

152

Mass spectrometry reveals nuclear SUMO targets and SUMO modified lysines of
Rhes
155   To identify the SUMO targets of Rhes, we subjected Ni-NTA enriched myc and myc-Rhes
156   samples (Fig. 1E) to SUMO peptide immunopurifications using a custom antibody that
157   recognizes the NQTGG remnant created on the modified lysine residue upon trypsin digestions.
158   SUMOylation site identification and quantified were obtained by MS analysis. This analysis
159   revealed numerous SUMOylated proteins and a significant increase of SUMOylation of at least
160   13 targets in myc-Rhes expressing cells compared to myc control (Fig. 1G, Data file S3).

161

162   Among the high-confidence SUMO substrates, we found Rhes increased the RapGEF5
163   SUMOylation at the lysine 422 and lysine 428 residues that are part of catalytic domain [49].
164   RapGEF5 is a direct target of 3'-5'-cyclic adenosine monophosphate (cAMP) and is involved in
165   cAMP-mediated signal transduction through activation of the Ras-like small GTPase RAPs:
166   RAP1A, RAP1B and RAP2A [50]. We found Rhes increased the SUMOylation at lysine 803 of
167   diacylglycerol kinase eta (DGKH), an enzyme that generate phosphatidic acid (PA) and activates
168   the Ras/B-Raf/C-Raf/MEK/ERK, We found Rhes also increased the SUMOylation of CCDC54

169 (the coiled coil domain containing protein 54), whose function is unknown, at lysine 318 (Fig.
170 1H).

171   Among the low confidence SUMO targets, we found that Rhes promoted the
172 SUMOylation of the SUMO-3 ligases PIASy (K59) and RanBP2 (K1605), as well as protein
173 polypbromo-1 (PBRM1, K1398, K1642), heterogenous nuclear ribonucleoprotein M (HNRNPM,
174 K145, K698), histone-lysine N-methyltransferase (SETDB1, K1032), RNA polymerase II-
175 associated factor 1 homolog (PAF1, K133) and mothers against decapentaplegic homolog 4
176 (SMAD4, K113) (Fig. 1H). Interestingly, Rhes is also one among the 4 high-confidence
177 SUMOylated targets. Rhes was found SUMOylated at six lysine residues 32, 110, 114, 120, 124
178 and 245 that spanned across the protein. The GTPase domain of Rhes contains 5 SUMO
179 modification sites and the C-terminal SUMO E3-like region harbors a SUMOylation site (Fig.
180 1I).

181   Together this data indicates that a) Rhes modulates SUMOylation of substrates involved
182 in cellular signaling and nuclear functions and b) Rhes is SUMOylated at multiple lysine
183 residues.

184

185 **Comparison of Rhes interactome and SUMOylation targets to further refine**
186 **potential new SUMO targets of Rhes**

187 Although the quantitative SUMO proteomic (Fig. 1) revealed novel putative SUMO targets of
188 Rhes, the number of SUMO candidates identified are relatively low. Such results are not entirely
189 unexpected because of the hurdles that are inherent to SUMOylation studies such as the low
190 abundance of the SUMO modified targets and the highly dynamic nature of SUMOylation.
191 Indeed, at any given time only <1% of the total protein are modified, further complicating their
192 identification [51]. Finally, SUMOylation of certain substrates in the native tissues such as
193 striatum may also be under the strict control of extracellular signaling.

194   Keeping all these limitations in perspective, we sought to identify the potential SUMO
195 targets further, using an unbiased approach. So, we applied four different filtering to sort out
196 SUMO substrates (Fig. 2A). First, we selected the common proteins by comparing Rhes
197 interactors in HEK293 cells [Fig. 1C, (*a*)] with all the SUMOylated proteins in Rhes expressing
198 HEK293 cells [Fig 1G, (*b*)] to obtain *a-1*. Second, we compared protein interactors of Rhes from
199 the striatum [9] (*c*) with the SUMOylated proteins in Rhes expressing HEK293 cells (*b*) and
200 obtained *b-1*. Third, we compared proteins interactor of Rhes in the striatum (*c*) with the SUMO
201 interacting proteins in the brain [52] (*d*), and obtained *c-1.* Fourth, we sorted shared protein
202 from *a-1*, *b-1* and *c-1* to obtain *d-1*. And fifth, we compared the high and low confidence SUMO

203 substrates of Rhes (*e-1*) with proteins identified from (*d-1*) to obtain *f-1* (Data file S4). This

204 approach has resulted in 27 novel targets that are SUMOylated as well as shown to interact with

205 Rhes (Fig. 2B). Most of these targets, such as histone deacetylase 1 (HDAC1), protein inhibitor of

206 activated STAT protein 4 (hPIASy or PIASy), histone-2B, (H2B), heterogeneous nuclear

207 ribonucleoprotein M (HNRNPM) and polybromo 1 (PBRM1) have roles in gene regulation,

208 indicating a strong nuclear function for Rhes.

209

210 **Rhes regulates SUMOylation of nuclear targets in cells**

211 Next we hypothesized that Rhes can directly modulate the SUMOylation of the targets identified

212 in Fig 2. To test this hypothesis, we selected certain targets (color coded) based on the already

213 available cDNA constructs from Addgene (Fig 2B). So, we carried out Ni-NTA denaturing

214 protocol, (Fig. 3) for these nuclear targets by expressing them in in HEK293 cells.

215 We found Rhes increased the SUMOylation of HDAC1 (Histone Deacetylase 1) and

216 histone 2 B, but it did not affect the SUMOylation of histone H2A.1 (Fig. 3A, B). Surprisingly

217 Rhes decreased the SUMOylation of HNRNPM, PBRM1 and PIASy (PIASy) SUMOylation (Fig.

218 3B, C). We could not detect SUMOylation of other targets, nucleophosmin (NPM), DGK, and

219 ribosomal protein L26 (RPL26) (Supplementary Fig. 1A). As expected, Rhes was readily

220 SUMOylated under these experimental conditions. Together this data indicates that Rhes

221 differentially modulates the SUMOylation of substrates that are involved in nuclear functions,

222 especially in regulation of gene expression.

223

224 **Rhes regulate the expression of genes involved in neuronal morphogenesis in the**

225 **striatum**

226 As Rhes differentially regulates the SUMOylation of nuclear targets implicated in the gene

227 expression, we hypothesized that Rhes may alter gene expression in the striatum *in vivo*. To

228 investigate this hypothesis, we isolated mRNA from WT and *Rhes$^{-/-}$* mice [RNA from 1 male and

229 1 female mouse was pooled per sample, triplicate for each group (WT or *Rhes$^{-/-}$*)] and carried

230 out high-throughput RNA seq analysis. We found that Rhes significantly altered the gene

231 expression profile in the striatum (Fig. 4A). Out of ~15,000 genes sequenced, 155 genes are

232 down-regulated, and 52 genes are up-regulated significantly in the striatum of *Rhes$^{-/-}$* mice

233 compared to WT control (Fig. 4A, Data file S5). Ingenuity pathway analysis (IPA) showed

234 molecular and cellular functions involved in cell morphology, cellular development, growth and

235 proliferation, and molecular transport are the major hits (Fig. 4B). For example, genes involved

236 in cell morphogenesis; for example, early growth response 2 (Egr2), necdin (Ndn), serum- and

7

237   glucocorticoid-regulated kinase 1 (Sgk1) and netrin-1 (Ntn1) are upregulated [53-57], and
238   neuropilin1 (Nrp1), basic-helix-loop helix 22 (Bhlhe22) and myocyte enhancer factor 2 (Mef2c)
239   are downregulated [58-62] (Fig 4A). A large majority of the genes, such as ephrin type-A
240   receptor 5 (Epha5) and slit guidance ligand 2 (Slit2), are unaffected. Using qPCR, we further
241   validated selected targets. We confirmed for example, Nrp1, Bhlhe22, Mef2c are downregulated,
242   Egr2 is upregulated, and exostosin glycosyltransferase 1 (Ext1) showed a decreased trend (P****
243   Value) in the striatum of *Rhes*$^{-/-}$ mice compare to WT striatum in qPCR analysis (Fig. 4C). This
244   data indicates that Rhes regulates the expression of genes involved in variety of biological
245   process with a prominent role in cellular morphology in the striatum.
246
247   **Rhes regulates a selected gene expression via SUMO**
248   Because Rhes regulates the SUMOylation of proteins such as HDAC1, HNRNPM, PBRM1 and
249   PIASy that are involved in gene expression, [63-68], we investigated if Rhes alters gene
250   expression via SUMO. We employed CRISPR/Cas-9 control (WT cells) and CRISPR/Cas-9
251   SUMO1/2/3 depleted striatal neuronal cells, that show ~60-70% of loss of SUMO (SUMO Δ
252   cells)[40]. To analyze the effect of Rhes on the expression of Ext1, Mef2c, Slit2, Epha5, and
253   Bhlhe22 in WT and SUMO Δ cells, cells were transfected with GFP or GFP-Rhes and sorted
254   using flow cytometry to obtain enriched population of cells expressing GFP or GFP-Rhes. While
255   Rhes increased the expression of Mef2c, Bhlhe22 in WT cells, it failed to do so in the SUMO Δ
256   cells (Fig. 4D). This result indicates that Rhes positively modulates the gene expression of
257   Bhlhe22 and Mef2c via SUMO. Rhes increased Epha5 and Ext1 in both the control and the
258   SUMO Δ cells, indicating that Rhes promotes Epha5 and Ext1 expression independent of SUMO
259   (Fig. 4D). Furthermore, while Slit2 is induced by Rhes in control cells, a high basal Slit2
260   expression was found in SUMO Δ cells that was not affected by Rhes expression (Fig. 4D).
261   Collectively, these results indicate Rhes regulates gene expression via SUMO dependent and
262   independent mechanisms.
263
264   **Rhes is enriched in the perinuclear membrane fractions**
265   As Rhes mostly regulates gene expression of selected nuclear targets, we investigated if Rhes is
266   localized in the nucleus. Using biochemical tools, we isolated and separated cytoplasmic and
267   nuclear fractions of the striatum from *Rhes*$^{+/+}$ and *Rhes*$^{-/-}$ mice (Fig. 5A). Using Western
268   blotting, we confirmed that Rhes is highly enriched in the nuclear fractions that is positive for
269   histone H3 (Fig. 5A). Rhes is also observed in the cytoplasmic fractions that are enriched for
270   cytoplasmic markers, mTOR, mitogen-activated protein kinase kinase (MEK) and lactate

8

271 dehydrogenase (LDH) (Fig. 5A). Since biochemically isolated subcellular fractions do not

272 unmistakably report the distribution of subcellular proteins, we sought to verify the localization

273 of Rhes using confocal fluorescence microscopy. Imaging analysis revealed that GFP-tagged-

274 Rhes is predominantly associated with perinuclear membranes and it is present at negligible

275 levels in the nucleus (Fig. 5B, red arrows). In addition to perinuclear localization, Rhes is also

276 enriched in the plasma membrane (Fig. 5B, yellow arrowhead), and membranous vesicles, as

277 consistent with our previous reports [40, 69]. Altogether, our result indicates that Rhes is

278 predominantly localized on the perinuclear membranes. We propose that Rhes may affect

279 SUMOylation of nuclear targets in the perinuclear location (Fig. 5C).

280

281 **DISCUSSION**

282 The data presented here demonstrate that a) Rhes is SUMOylated on multiple lysine

283 sites; b) Rhes regulates the SUMOylation of nuclear proteins, and c) Rhes regulates gene

284 expression in the striatum at least partly via SUMO-mediated mechanisms. Importantly, despite

285 that, it is well known that Rhes is post-translationally modified *in vivo* [9, 70]; however, the

286 nature of modification remained unknown. This study indicates that SUMO may contribute to

287 such *in vivo* Rhes modification.

288 Interestingly, the presence of multiple closely spaced SUMO modification sites on Rhes

289 on K110, K114, K120, K124 indicates that these residues may act as anchors that can associate

290 with SUMO-interacting motif (SIM) which are known to be involved in protein-protein

291 interaction [71, 72]. Such closely spaced SUMOylation events are also found on other SUMO E3

292 ligases such as PIAS1 lysines K40, K46, K56, and K58 and PIASy lysines K59 and K69, K128 and

293 K135; and RanBP2 K1596 and K1605, K2513 and K2531, and K2571 and K2592 [73, 74]. Thus,

294 multiple lysine SUMO modifications appear to be a characteristic feature across many SUMO E-

295 3 like proteins. Identifying the role of each lysine modification, and whether Rhes auto-

296 SUMOylates itself or if other potential SUMO E3 ligases SUMOylate Rhes needs further

297 investigation.

298 Intriguingly, we report that Rhes differentially alters the SUMOylation of SUMO E3

299 ligases. Rhes decreased the overall SUMOylation on PIAS in the cells (Fig. 3B), while promoting

300 the specific SUMOylation of PIASy on lysine 59 (Fig. 1H). Similarly, MS analysis revealed that

301 Rhes significantly increases the SUMOylation of RanBP2 on lysine 1605, but not on lysine 2592

302 (Fig 2A, Data file S5). These results indicate that Rhes may differentially affect the SUMOylation

303 of SUMO E3 ligase(s) on selected lysine targets. In the future, it will be interesting to test

304 whether PIASy or RanBP2 can act as SUMO E3 ligase for Rhes. Even though it is known that

9

305 SUMOylation modifies SUMO E3 ligases, the biological significance of such modifications

306 remains less understood. Previously, we reported that Rhes promoted cross-SUMOylation

307 between SUMO E1 (Aos/Uba9) and E2 (Ubc9) ligases and predicted such regulation might work

308 as "symbiotic" regulation between two evolutionarily conserved SUMO E1 and E2 enzymes [44].

309 Based on the data presented here, we propose that Rhes may also promote reciprocal and

310 symbiotic regulations between SUMO E3 ligases through SUMO modification that may have a

311 significant impact on regulating complex cellular and behavioral functions of the striatum via

312 protein-protein interactions [9].

313 The results presented here clearly indicate that Rhes is involved in the regulation of gene

314 expression in the striatum, intriguingly, it can both increase and decrease gene expression in the

315 striatum. A previous independent study also reported that Rhes might inhibit gene expression

316 by acting as a cis-modulator [75], but the mechanisms were unclear. It is well established that

317 SUMOylation participates in cis-regulation and is involved in both transcriptional repression as

318 well as activation functions [51, 76, 77]. As Rhes KO cells show overall diminished SUMOylation

319 in the striatum [44] and altered gene expressions, we predict that the Rhes-SUMO pathway may

320 regulate gene expression as cis-modulator, for example via the SUMOylation of transcription

321 factors. Consistent with this notion, although we did not observe a significance alteration of

322 HDAC1 SUMOylation on lysine 89 or lysine 476 in our proteomics analysis (Data S3),

323 presumably due to low stoichiometry, we found that Rhes enhances the SUMOylation of HDAC1

324 in our biochemical experiments (Fig. 2B).   Thus Rhes may alter HDAC1 activity via

325 SUMOylation at lysine 89 and lysine 476, a catalytically essential residue involved in the gene

326 repression [78-80].

327 Previous studies indicate that SUMOylation of H2B is involved in the repression of gene

328 expression [81]. Because we found that Rhes increases the SUMOylation of H2B (Fig. 3), which

329 is SUMOylated at multiple lysine (Data file S4), including previously reported, lysine 6 [81], we

330 propose that Rhes-SUMO pathway may affect gene expression via more than one nuclear

331 targets.

332 The cellular compartment in which Rhes regulates the SUMOylation of nuclear proteins

333 remains to be elucidated. Since we found that Rhes is enriched on the perinuclear space (Fig.

334 5B), we predict that this location may serve as the prime site for SUMOylation of proteins (Fig.

335 5C). In support of this notion, previous studies showed that SUMO E3 ligase RanBP2 localized

336 on the perinuclear location [the cytoplasmic side of nuclear pore complex (NPC)], which

337 regulates import and export of proteins, and mediates global gene expression in cell models [82,

338 83]. RanBP2 also enhances the SUMOylation of HDAC4 and HNRNPM proteins, which are

339 involved in mRNA splicing and transport [84, 85]. Although the localization of Rhes on the NPC

340 is not currently documented, we found that Rhes coimmunoprecipitates with RanBP2 and

341 Sec13, two known components of the NPC. Rhes has been shown to interact with NPC associated

342 proteins during motor stimulation in the striatum, including HNRNP (L1 and H2 isoforms) [9].

343 Thus, we predict that Rhes may associate with the NPC to regulate the SUMOylation of targets

344 involved in gene regulation as well as mRNA splicing, a process shown to require SUMOylation

345 [86]. In addition, Rhes may alter SUMO-independent signaling, such as the modulation of

346 mTOR and PKA signaling pathways that are linked to gene expression [6, 8, 87-89].

347   Our finding demonstrates that Rhes alters the expression of genes involved in cell

348 morphology and differentiation (Fig. 4) and is a potent inducer of TNT-like cellular protrusions

349 [40]. We propose that Rhes may mediate TNT-like protrusions and cell-to-cell transport of

350 cargoes via the regulation of the expression of transcription factors such as Mecf2, Egr2,

351 Bhlhe22, which are known regulators of neuronal morphology and differentiation in a SUMO

352 dependent manner. Consistent with this notion, depletion of SUMO diminishes the formation of

353 TNT-like protrusions [40] and cell-to-cell transport as well as alters Rhes mediates expression

354 of Mef2c and Bhlhe22-1 9 (Fig. 4).

355   Collectively, by combining high throughput interactomics, SUMO proteomics, gene

356 expression analysis, and biochemical tools, we demonstrate that Rhes promotes the

357 SUMOylation of nuclear substrates that are involved in gene expression. Thus, Rhes may impact

358 striatal function and dysfunction associated with neurological and neurodegenerative disease via

359 the SUMO-mediated regulation of gene expression.

360

361 **MATERIALS AND METHODS**

362 ***Reagents, Plasmids and Antibodies***

363 Unless otherwise noted, reagents were obtained from Sigma. Full length Rhes cDNA constructs,

364 Myc, GST or GFP tagged, were cloned in pCMV vectors (Clontech) [11, 12, 40].. Mass

365 spectrometry detection compatible His6-mSUMO1, His6-mSUMO2 and His6-mSUMO3 were

366 cloned as described [90, 91]. p181 pK7-HDAC1 (GFP) (Addgene; 11054) were from Ramesh

367 Shivdasani. H2B-mCherry (Addgene; 20972) were from Robert Benezra. mH2A1.2-CT-GFP

368 (Addgene, 45169) were from Brian Chadwick, Hunt Willard. pT7-V5-SBP-C1-HshnRNPM

369 (Addgene; 64924) were from Elisa Izaurralde. GFP-PBRM1 (Addgene; 65387) were from Kyle

370 Miller. Flag-hPIASy (Addgene; 15208) were from Ke Shuai. GFP-NPM WT (Addgene; 17578)

371 were from Xin Wang. DGK beta (Addgene; 35405) were from Robert Lefkowitz and Stephen

372 Prescott. pCMV-L26-Flag (Addgene; 19972) were from Moshe Oren. 6x-His Tag Antibody (clone

373   HIS.H8) (1:1000, # MA1-21315) was from ThermoFisher Scientific. Antibodies for GST-HRP

374   (1:5000, #sc-138), and Myc (1:3000, #sc-40) were obtained from Santa Cruz Biotechnology.

375   mCherry antibody (1:1000, NBP2-25157) was from Novus Biologicals. Flag antibody (1:1000,

376   F7425) was obtained from Sigma-Aldrich. HA.11 Epitope Tag Antibody (1:1000, 901513) was

377   from BioLegend (previously Covance catalog# MMS-101R). V5-Tag (1:1000, #13202), GFP

378   (1:1000, #2956), mTOR (1:3000, #2983), Histone H3 (1:10,000, #4499), MEK1/2 (1:1000,

379   #8727) and LDH (1:5000, #2012) were from Cell Signaling Technology, Inc. Rhes antibody

380   (1:1000, RHES-101AP) was from Fabgennix.

381

382   ***Ni-NTA Denaturing Pull Down***

383   Ni-NTA pull down of His-SUMO conjugates was performed as previously described [12, 92].

384   Briefly, HEK293 cells (expressing transfected His-SUMO mutant and indicated constructs) were

385   pretreated with MG132 (25 μM, 4 hr), rinsed in PBS, scraped from 10cm^2 dishes, and

386   centrifuged at 750 x g for 5 min. Cell pellets were then directly lysed in Pull Down Buffer [6 M

387   Guanidine hydrochloride, 10 mM Tris, 100 mM sodium phosphate, 40 mM imidazole, 5 mM β-

388   mercaptoethanol (β-ME), pH 8.0] and sonicated. Lysates were then clarified by centrifugation at

389   3,000 x g for 15 minutes. All subsequent wash steps were performed with 10 resin volumes of

390   buffer followed by centrifugation at 800 x g for 2 min. Ni-NTA Agarose beads (#30210; Qiagen)

391   were pre-equilibrated by washing three times with Pull Down Buffer. After equilibration, beads

392   were resuspended in Pull Down Buffer as a 50% slurry of beads to buffer. After protein

393   quantification of cell lysates, 1 mg of lysate was added to 40 μL of Ni-NTA bead slurry to a total

394   volume of 1 mL in microcentrifuge tubes. Beads were then incubated overnight at 4°C mixing

395   end over end. The following day, beads were centrifuged and underwent washing once in Pull

396   Down Buffer, once in pH 8.0 Urea Buffer (8 M Urea, 10 mM Tris, 100 mM sodium phosphate,

397   0.1% Triton X-100, 20 mM imidazole, 5 mM β-ME, pH 8.0), and three additional times in pH

398   6.3 Urea Buffer (8 M Urea, 10 mM Tris, 100 mM sodium phosphate, 0.1% Triton-X100, 20 mM

399   imidazole, 5 mM β-ME, pH 6.3). Elution was performed using 20 μL of Elution Buffer (pH 8.0

400   Urea Buffer containing 200 mM imidazole, 4X NuPAGE LDS loading dye, 720 mM β-ME).

401   Samples were then heated at 100°C for 5 minutes and directly used for Western Blotting. Inputs

402   were loaded as 1% of the total cell lysate. The SUMOylation is quantified by normalizing the

403   intensity of SUMOylation bands to the respective unmodified bands using Image-J.

404

405   ***GFP-Rhes localization studies***

406 Approximately 75,000 STHdh$^{Q111/Q111}$ cells were seeded on 35mm glass bottom dishes. After 24h
407 the cells were transfected with indicated plasmids. Cells were imaged live using a Zeiss 880
408 confocal microscope at 63X oil immersion Plan- apochromat objective (1.4 NA).
409

410 ***Purification of SUMOylated Rhes interacting proteins***
411 Proteins extracts from GST + mSUMO3, and GST-Rhes + mSUMO3 expressing HEK298 cells
412 were purified with glutathione beads to recover global Rhes interacting partners. The resulting
413 purified material was subjected to denaturing Ni-NTA purification step to enrich for the
414 SUMOylated interacting parteners. The Ni-NTA bound material was digested with trypsin,
415 desalted on C-18 and analyzed by LC-MS, as described before [47, 93, 94].

416 ***SUMO peptide enrichment and MS detection***
417 SUMOylated proteins were enriched from myc + mSUMO3 or myc-Rhes + mSUMO3 expressing
418 HEK293 cells using Ni-NTA. The solid support bound material was digested on the Ni-NTA
419 beads with trypsin and the resulting peptides desalted on C-18 cartridges. SUMOylated peptides
420 were immunopurified with the anti-NQTGG antibody that recognizes the NQTGG remnant
421 exposed on the SUMOylated lysine upon tryptic digestion. SUMO site quantification and
422 quantification was carried out with MaxQuant, as described before [46, 94, 95].
423

424 ***SUMO1/2/3 Knockout in striatal Cells.*** Striatal cells deleted for SUMO1, 2 and 3 is using
425 CRISPR/Cas9 SUMO gRNAs as described [40].
426

427 ***Mice.*** For fractionation experiments, we used Rhes KO (*Rhes$^{-/-}$*) mice, and C57BL/6J mice.
428 Rhes KO mice were obtained from Alessandro Usiello and were backcrossed with C57BL/6J
429 mice at least 8 generations; homozygous Rhes KO were used for all of the experiments [9, 13].
430 WT mice (C57BL/6) were obtained from Jackson Laboratory and maintained in our animal
431 facility according to Institutional Animal Care and Use Committee at The Scripps Research
432 Institute.
433

434 ***Nuclear and Cytoplasmic Separation from striatum***
435 Striatum from C57BL/6J and Rhes KO mice was fractionated using the nuclear/cytosol
436 fractionation kit according to the manufacturer's instructions with minor modifications
437 (BioVision). Briefly, striatum from C57BL/6J and Rhes KO mice was rapidly dissected out and
438 homogenized in CEB (cytosolic extraction buffer)-A with DTT and protease inhibitor, and
439 incubating for 10 min on ice prior to addition of CEB-B. The lysates were vortexed for 5 sec and

13

440   incubated on ice for 1 min. The lysates were then centrifuged at 4°C for 5 min at 16,000 x g in a

441   microcentrifuge. And the supernatants were kept as the cytoplasmic fraction. The nuclear pellet

442   was resuspended in NEB (nuclear extraction buffer). And vortexed the lysates for 15 sec. This

443   step was repeated 5 times every 10 min. The nuclear pellet was centrifuged at 4°C for 10 min at

444   16,000 x g in a microcentrifuge. And the supernatants were kept as the nuclear fraction. The

445   protein concentration was determined in the cytoplasmic and nuclear fractions using the BCA

446   Protein Assay Kit (Pierce, Rockford, IL, USA). Equivalent amounts of protein samples (50 µg)

447   were resolved by SDS-PAGE followed by immunoblotting as described below.

448

449   ***Western blotting***

450   Equal amounts of protein (20-50 µg) were loaded and were separated by electrophoresis in 4 to

451   12% Bis-Tris Gel (Thermo Fisher Scientific), transferred to polyvinylidene difluoride

452   membranes, and probed with the indicated antibodies. HRP-conjugated secondary antibodies

453   (Jackson ImmunoResearch Inc.) were probed to detect bound primary IgG with a

454   chemiluminescence imager (Alpha Innotech) using enhanced chemiluminescence from

455   WesternBright Quantum (Advansta).   Where indicated the membranes were stained for

456   ponceau.

457

458   ***Global mRNA-seq from WT and Rhes KO striatum***

459   WTor Rhes KO mice striatum [1 male and 1 female (pooled), in triplicate were lysed in Trizol

460   reagent. RNA was extracted from miRNeasy kit from Qiagen (cat. No. 217004) and mRNA-seq

461   was performed as described before [96].

462

463   ***qPCR validation of targets***

464   Striatum of mice (WT or Rhes KO) lysed in Trizol reagent. 250 ng RNA was used to prepare

465   cDNA using Takara primescript kit (Cat no. 6110A) using random hexamers. The qRT-PCR of

466   genes was performed with SYBR green (Takara RR420A) reagents. Primers for all the genes

467   were designed based on sequences available from the Harvard qPCR primer bank. The primer

468   sequences are as follows:

469   *Gapdh* mouse (Forward primer) 5' primer AGGTCGGTGTGAACGGATTTG

470   (Reverse primer) 3' primer TGTAGACCATGTAGTTGAGGTCA

471   *Nrp1* mouse (Forward primer) 5' primer GACAAATGTGGCGGGACCATA

472   (Reverse primer) 3' primer TGGATTAGCCATTCACACTTCTC

14

473   *Bhlhe22* mouse (Forward primer) 5' primer TGAACGACGCTCTGGATGAG

474   (Reverse primer) 3' primer GGTTGAGGTAGGCGACTAAGC

475   *Slit2* mouse (Forward primer) 5' primer GGCAGACACTGTCCCTATCG

476   (Reverse primer) 3' primer GTGTTGCGGGGGATATTCCT

477   *Epha5* mouse (Forward primer) 5' primer AAGGAACCCTGTGGCTATTGG

478   (Reverse primer) 3' primer GCAAACATGCCCGTTTTAGAGAA

479   *Dcx* mouse (Forward primer) 5' primer CATTTTGACGAACGAGACAAAGC

480   (Reverse primer) 3' primer TGGAAGTCCATTCATCCGTGA

481   *Ext1* mouse (Forward primer) 5' primer TGGAGGCGTGCAGTTTAGG

482   (Reverse primer) 3' primer GAAGCGGGGCCAGAAATGA

483   *Egr2* mouse (Forward primer) 5' primer GCCAAGGCCGTAGACAAAATC

484   (Reverse primer) 3' primer CCACTCCGTTCATCTGGTCA

485   *Mef2c* mouse (Forward primer) 5' primer ATCCCGATGCAGACGATTCAG

486   (Reverse primer) 3' primer AACAGCACACAATCTTTGCCT

487   *Plxna1* mouse (Forward primer) 5' primer GGGTGTGTGGATAGCCATCAG

488   (Reverse primer) 3' primer GCCAACATATACCTCTCCTGTCT

489   *Met* mouse (Forward primer) 5' primer GTGAACATGAAGTATCAGCTCCC

490   (Reverse primer) 3' primer TGTAGTTTGTGGCTCCGAGAT

491   *Efna5* mouse (Forward primer) 5' primer ACACGTCCAAAGGGTTCAAGA

492   (Reverse primer) 3' primer GTACGGTGTCATTTGTTGGTCT

493

Bioinformatics and statistical analysis of data analysis of proteomics

494

495 Normalized gene counts were averaged and log10 transformed for WT and Rhes KO samples

496 and were plotted against each other where Rhes Ko log10 mean values were on x-axis and WT

497 log10 mean values were on y-axis. Differentially regulated genes were identified using padj

498 <0.05 cut off and up (higher in Rhes KO) and down (higher in WT) regulated genes were

499 marked with green and red respectively. The graph was generated using JMP®, Version 13.2.1.

500 SAS Institute Inc., Cary, NC.

501

Statistical Analysis

502

503 Data were expressed as means ± SEM. All of the experiments were performed at least in

504 triplicate and repeated twice at minimum. Statistical analysis was performed using Student's *t*

505   test or one-Way ANOVA followed by Newman-Keuls multiple comparison test (GraphPad Prism
506   7).

507

508   ***Data availability***

509   Sequencing data have been submitted to the Gene Expression Omnibus (GEO) data repository,
510   under the accession number GSE150990.

511

512   **LEGENDS**

513   **Fig 1. Interactome and SUMO proteome identifies putative SUMO substrates of**
514   **Rhes** (**A**) Western blot of HEK293 cells expressing His-SUMO 1m, His-SUMO 2m, or His-
515   SUMO 3m**.** (**B**) Western blot for indicated proteins after glutathione-affinity pulldown in
516   HEK293 cells expressing GST + His-mSUMO3 (control) or GST-Rhes + His-mSUMO3 and
517   corresponding input (5%) for the indicated proteins. (**C**) Volcano plot of proteins bound to
518   affinity purified GST-Rhes (Rhes) co-expressing mSUMO3, compared to affinity purified GST
519   co-expressing mSUMO3 (control), identified by LC-MS/MS in biological triplicate. (**D**) Volcano
520   plot of SUMOylated proteins that are bound to glutathione enriched GST-Rhes (Rhes)+ His-
521   mSUMO3, compared to glutathione enriched GST + His-mSUMO3 (control) vs. GST-Rhes co-
522   expressing mSUMO3, identified by LC-MS/MS in biological triplicate. (**E**) Western blot of His-
523   tagged SUMO enrichment using Ni-NTA TALON beads in HEK293 cells expressing myc + His-
524   mSUMO3 or myc-Rhes + His- mSUMO3. S*Rhes represents SUMOylated Rhes. (**F**)
525   Quantification of overall SUMOylation in Ni-NTA enriched, myc + His- mSUMO3 or myc-Rhes
526   + His-mSUMO3. Data represents means ± SEM, (n =3), ***P < 0.001, Student's t test. (**G**)
527   Volcano plot of SUMOylation site changes in myc-Rhes + His-mSUMO3 compared to myc +
528   His-mSUMO3 (control), identified by LC-MS/MS in biological triplicate. (**H**) High and low
529   confidence SUMO substrates of Rhes identified in *(G)*. (**I**) Representation of Rhes domains with
530   mapping of the SUMO sites identified.

531   **Fig 2. Flow chart to identify potential SUMOylated proteins.** (**A**) Proteins that interacts
532   with Rhes in His-mSUMO3 overexpression *(a)* are compared with all the SUMOylated proteins
533   *(b)* and obtained *(a-1)*. Rhes interactors in the striatum, Shahani, 2016[9] *(c)* are compared with
534   *(b) to* obtain *(b-1)*. Then, *(a)* is compared with SUMOylated proteins in the brain, Matsuzaki,
535   2015[52], *(d)* to obtain *(c-1)*. Later, a-1, b-1 and c-1 are compared to obtain d-1. (**B**) Finally, the
536   high and low confidence SUMO substrates of Rhes *(e-1)* were compared to d-1 to generate a list
537   of the top 27 putative SUMO substrates of Rhes *(f-1)*.

16

Fig 3. Rhes regulates the SUMOylation of nuclear targets. (**A**) Western blot of Ni-NTA enrichment of SUMOylated proteins (S*) from the lysates obtained from HEK293 cells expressing myc + His-mSUMO3 or myc-Rhes + His-mSUMO3 constructs either with GFP-HDAC1, m-cherry H2B or GFP-H2A1.2. (**B**). Bar graphs indicates quantification of SUMOylation (%) from (A). Data represents mean ± SEM, (n =3), *$P < 0.05$, **$P < 0.01$, Student's *t* test. n.s: not significant. (**C**) Western blot of Ni-NTA enrichment of SUMOylated proteins from the lysates obtained from HEK293 cells expressing myc + His-mSUMO3 or myc-Rhes + His-mSUMO3 constructs either with V5-HNRNPM1, GFP-PBRM1 or Flag-PIASy. (**D**). Bar graphs indicates quantification of SUMOylation (%) from (C). Data represents mean ± SEM, (n =3), **$P < 0.01$, ****$P < 0.0001$, Student's *t* test.

Fig 4. Rhes regulates genes involved in cellular differentiation and morphogenesis via SUMOylation. (**A**) Mean normalized counts of gene expression based on RNA seq data from Rhes KO vs. WT mice striatum. (**B**) IPA analysis of the molecular and cellular functions altered in striatum of Rhes KO mice compared to WT mice from (A). (**C**) Expression of indicated genes (normalized to *Gapdh*), involved in cell morphology and cellular development were validated by qPCR in Rhes KO vs. WT mice striatum. Error bar represents mean ± SEM, (n =3), *$P < 0.05$, **p<0.01 by Student-*t* test. (**D**) Gene expression data for the indicated genes (normalized to *Gapdh*) in WT or SUMO1,2,3 KO (Δ) cells to assess the effect of SUMOylation in presence of GFP or GFP-Rhes. Error bar represents mean ± SEM, (n =3), *$P < 0.05$, **$P < 0.01$ compared to GFP in WT. ##$P < 0.01$ between Rhes in WT and Rhes in SUMO1,2,3 Δ cells by One-Way ANOVA followed by Newman-Keuls multiple comparison test.

Fig 5. Rhes is preferentially localized around the perinuclear membrane. (**A**) Subcellular localization of Rhes was assessed in cytosolic and nuclear fractions from Rhes KO (*Rhes^{-/-}*) vs. WT (*Rhes^{+/+}*) mice striatum. The cytosolic markers MEK and LDH and the nuclear marker Histone H3 were probed to validate proper cellular fractionation. (**B**) Representative confocal and brightfield (DIC) image of striatal neuronal cell expressing GFP-Rhes, indicating the localization of Rhes on nuclear membrane and perinuclear space. Inset shows the boxed area at higher magnification. White arrows indicate perinuclear localization of Rhes, and yellow arrowhead indicates the localization of Rhes on plasma membrane. (**C**) Model depicting that Rhes can SUMOylate its targets, including HDAC1, in the cytoplasm and promotes its entry into the nucleus to regulate gene expression.

17

569 **Supplementary Figure 1.** Western blot of Ni-NTA enrichment of SUMOylated proteins from
570 lysates obtained from HEK293 cells expressing myc + His- mSUMO3 or myc-Rhes + His-
571 mSUMO3 constructs either with GFP-NPM, HA-DGK-β or Flag-L26.

572 **Author contributions:** S. Su conceptualized and designed the project. O.R carried out all the
573 biochemical SUMO work. M. S carried out mRNA seq, qPCR, SUMO-KO cell generation and
574 confocal microscopy. N.S carried out biochemical separation of Rhes. UNRJ assisted in mRNA
575 seq and cell culture experiments. F. M and T.P designed the mass spec (MS) compatible his-
576 mSUMO3 construct and carried out MS analysis of Rhes interactors and identification of
577 SUMO. G.C assisted in bioinformatics. P.K generated mRNA seq library and sequencing. S.Su
578 wrote the paper with input from the co-authors.

585
586
587

588 **REFERENCES**

589 1   Harrison, L. M. (2012) Rhes: a GTP-binding protein integral to striatal physiology and
590 pathology. Cell Mol Neurobiol. **32**, 907-918
591 2   Usui, H., Falk, J. D., Dopazo, A., de Lecea, L., Erlander, M. G. and Sutcliffe, J. G. (1994)
592 Isolation of clones of rat striatum-specific mRNAs by directional tag PCR subtraction. J Neurosci.
593 **14**, 4915-4926
594 3   Sciamanna, G., Napolitano, F., Pelosi, B., Bonsi, P., Vitucci, D., Nuzzo, T., Punzo, D.,
595 Ghiglieri, V., Ponterio, G., Pasqualetti, M., Pisani, A. and Usiello, A. (2015) Rhes regulates
596 dopamine D2 receptor transmission in striatal cholinergic interneurons. Neurobiol Dis. **78**, 146-
597 161
598 4   Vargiu, P., De Abajo, R., Garcia-Ranea, J. A., Valencia, A., Santisteban, P., Crespo, P. and
599 Bernal, J. (2004) The small GTP-binding protein, Rhes, regulates signal transduction from G
600 protein-coupled receptors. Oncogene. **23**, 559-568
601 5   Errico, F., Santini, E., Migliarini, S., Borgkvist, A., Centonze, D., Nasti, V., Carta, M., De
602 Chiara, V., Prosperetti, C., Spano, D., Herve, D., Pasqualetti, M., Di Lauro, R., Fisone, G. and
603 Usiello, A. (2008) The GTP-binding protein Rhes modulates dopamine signalling in striatal
604 medium spiny neurons. Mol Cell Neurosci. **37**, 335-345

605   6   Ghiglieri, V., Napolitano, F., Pelosi, B., Schepisi, C., Migliarini, S., Di Maio, A., Pendolino,
606   V., Mancini, M., Sciamanna, G., Vitucci, D., Maddaloni, G., Giampa, C., Errico, F., Nistico, R.,
607   Pasqualetti, M., Picconi, B. and Usiello, A. (2015) Rhes influences striatal cAMP/PKA-dependent
608   signaling and synaptic plasticity in a gender-sensitive fashion. Sci Rep. **5**, 10933

609   7   Harrison, L. M. and He, Y. (2011) Rhes and AGS1/Dexras1 affect signaling by dopamine
610   D1 receptors through adenylyl cyclase. J Neurosci Res. **89**, 874-882

611   8   Subramaniam, S., Napolitano, F., Mealer, R. G., Kim, S., Errico, F., Barrow, R., Shahani,
612   N., Tyagi, R., Snyder, S. H. and Usiello, A. (2011) Rhes, a striatal-enriched small G protein,
613   mediates mTOR signaling and L-DOPA-induced dyskinesia. Nat Neurosci. **15**, 191-193

614   9   Shahani, N., Swarnkar, S., Giovinazzo, V., Morgenweck, J., Bohn, L. M., Scharager-Tapia,
615   C., Pascal, B., Martinez-Acedo, P., Khare, K. and Subramaniam, S. (2016) RasGRP1 promotes
616   amphetamine-induced motor behavior through a Rhes interaction network ("Rhesactome") in
617   the striatum. Sci Signal. **9**, ra111

618   10   Eshragi, M., Ramirez Jarquin, U. N., Shahani, N., Swarnkar, S., Galli, N., Rivera, O.,
619   Tsaprailis, G., Scharager-Tapia, C., Crynen, G., Usiello, A. and Subramaniam, S. (2019) RasGRP1
620   is a Causal Factor in the Development of L-DOPA-induced dyskinesia in Parkinson Disease.
621   Science Advances. **In press**

622   11   Mealer, R. G., Murray, A. J., Shahani, N., Subramaniam, S. and Snyder, S. H. (2014) Rhes,
623   a striatal-selective protein implicated in Huntington disease, binds beclin-1 and activates
624   autophagy. J Biol Chem. **289**, 3547-3554

625   12   Subramaniam, S., Sixt, K. M., Barrow, R. and Snyder, S. H. (2009) Rhes, a striatal specific
626   protein, mediates mutant-huntingtin cytotoxicity. Science. **324**, 1327-1330

627   13   Swarnkar, S., Chen, Y., Pryor, W. M., Shahani, N., Page, D. T. and Subramaniam, S. (2015)
628   Ectopic expression of the striatal-enriched GTPase Rhes elicits cerebellar degeneration and an
629   ataxia phenotype in Huntington's disease. Neurobiol Dis. **82**, 66-77

630   14   Okamoto, S., Pouladi, M. A., Talantova, M., Yao, D., Xia, P., Ehrnhoefer, D. E., Zaidi, R.,
631   Clemente, A., Kaul, M., Graham, R. K., Zhang, D., Vincent Chen, H. S., Tong, G., Hayden, M. R.
632   and Lipton, S. A. (2009) Balance between synaptic versus extrasynaptic NMDA receptor activity
633   influences inclusions and neurotoxicity of mutant huntingtin. Nat Med. **15**, 1407-1413

634   15   Seredenina, T., Gokce, O. and Luthi-Carter, R. (2011) Decreased striatal RGS2 expression
635   is neuroprotective in Huntington's disease (HD) and exemplifies a compensatory aspect of HD-
636   induced gene regulation. PLoS One. **6**, e22231

637   16   Baiamonte, B. A., Lee, F. A., Brewer, S. T., Spano, D. and LaHoste, G. J. (2013)
638   Attenuation of Rhes activity significantly delays the appearance of behavioral symptoms in a
639   mouse model of Huntington's disease. PLoS One. **8**, e53606

640   17   Sbodio, J. I., Paul, B. D., Machamer, C. E. and Snyder, S. H. (2013) Golgi protein ACBD3
641   mediates neurotoxicity associated with Huntington's disease. Cell Rep. **4**, 890-897

642   18   Lu, B. and Palacino, J. (2013) A novel human embryonic stem cell-derived Huntington's
643   disease neuronal model exhibits mutant huntingtin (mHTT) aggregates and soluble mHTT-
644   dependent neurodegeneration. FASEB J. **27**, 1820-1829

645   19   Argenti, M. (2014) THE ROLE OF MITOCHONDRIAL DYSFUNCTION IN HUNTINGTON'S
646   DISEASE PATHOGENESIS AND ITS RELATION WITH STRIATAL RHES PROTEIN. Ph.D Thesis,
647   Università degli Studi di Padova, Padova PD, Italy

648 20   Lee, J. H., Tecedor, L., Chen, Y. H., Monteys, A. M., Sowada, M. J., Thompson, L. M. and
649 Davidson, B. L. (2015) Reinstating aberrant mTORC1 activity in Huntington's disease mice
650 improves disease phenotypes. Neuron. **85**, 303-315

651 21   Hernandez, I., Luna, G., Rauch, J. N., Reis, S. A., Giroux, M., Karch, C. M., Boctor, D.,
652 Sibih, Y. E., Storm, N. J., Diaz, A., Kaushik, S., Zekanowski, C., Kang, A. A., Hinman, C. R., Cerovac,
653 V., Guzman, E., Zhou, H., Haggarty, S. J., Goate, A. M., Fisher, S. K., Cuervo, A. M. and Kosik, K. S.
654 (2019) A farnesyltransferase inhibitor activates lysosomes and reduces tau pathology in mice
655 with tauopathy. Sci Transl Med. **11**

656 22   Vadgama, N., Pittman, A., Simpson, M., Nirmalananthan, N., Murray, R., Yoshikawa, T.,
657 De Rijk, P., Rees, E., Kirov, G., Hughes, D., Fitzgerald, T., Kristiansen, M., Pearce, K., Cerveira, E.,
658 Zhu, Q., Zhang, C., Lee, C., Hardy, J. and Nasir, J. (2019) De novo single-nucleotide and copy
659 number variation in discordant monozygotic twins reveals disease-related genes. Eur J Hum
660 Genet. **27**, 1121-1133

661 23   Rustom, A., Saffrich, R., Markovic, I., Walther, P. and Gerdes, H. H. (2004) Nanotubular
662 highways for intercellular organelle transport. Science. **303**, 1007-1010

663 24   Austefjord, M. W., Gerdes, H. H. and Wang, X. (2014) Tunneling nanotubes: Diversity in
664 morphology and structure. Commun Integr Biol. **7**, e27934

665 25   Gousset, K., Marzo, L., Commere, P. H. and Zurzolo, C. (2013) Myo10 is a key regulator
666 of TNT formation in neuronal cells. J Cell Sci. **126**, 4424-4435

667 26   Vignais, M. L., Caicedo, A., Brondello, J. M. and Jorgensen, C. (2017) Cell Connections by
668 Tunneling Nanotubes: Effects of Mitochondrial Trafficking on Target Cell Metabolism,
669 Homeostasis, and Response to Therapy. Stem Cells Int. **2017**, 6917941

670 27   Dupont, M., Souriant, S., Lugo-Villarino, G., Maridonneau-Parini, I. and Verollet, C.
671 (2018) Tunneling Nanotubes: Intimate Communication between Myeloid Cells. Front Immunol.
672 **9**, 43

673 28   Panasiuk, M., Rychlowski, M., Derewonko, N. and Bienkowska-Szewczyk, K. (2018)
674 Tunneling Nanotubes as a Novel Route of Cell-to-Cell Spread of Herpesviruses. J Virol. **92**

675 29   Keller, K. E., Bradley, J. M., Sun, Y. Y., Yang, Y. F. and Acott, T. S. (2017) Tunneling
676 Nanotubes are Novel Cellular Structures That Communicate Signals Between Trabecular
677 Meshwork Cells. Invest Ophthalmol Vis Sci. **58**, 5298-5307

678 30   Delage, E., Cervantes, D. C., Penard, E., Schmitt, C., Syan, S., Disanza, A., Scita, G. and
679 Zurzolo, C. (2016) Differential identity of Filopodia and Tunneling Nanotubes revealed by the
680 opposite functions of actin regulatory complexes. Sci Rep. **6**, 39632

681 31   Zhu, H., Xue, C., Xu, X., Guo, Y., Li, X., Lu, J., Ju, S., Wang, Y., Cao, Z. and Gu, X. (2016)
682 Rab8a/Rab11a regulate intercellular communications between neural cells via tunneling
683 nanotubes. Cell Death Dis. **7**, e2523

684 32   Desir, S., Dickson, E. L., Vogel, R. I., Thayanithy, V., Wong, P., Teoh, D., Geller, M. A.,
685 Steer, C. J., Subramanian, S. and Lou, E. (2016) Tunneling nanotube formation is stimulated by
686 hypoxia in ovarian cancer cells. Oncotarget. **7**, 43150-43161

687 33   Polak, R., de Rooij, B., Pieters, R. and den Boer, M. L. (2015) B-cell precursor acute
688 lymphoblastic leukemia cells use tunneling nanotubes to orchestrate their microenvironment.
689 Blood. **126**, 2404-2414

690 34   Burtey, A., Wagner, M., Hodneland, E., Skaftnesmo, K. O., Schoelermann, J., Mondragon,
691 I. R., Espedal, H., Golebiewska, A., Niclou, S. P., Bjerkvig, R., Kogel, T. and Gerdes, H. H. (2015)

692   Intercellular transfer of transferrin receptor by a contact-, Rab8-dependent mechanism
693   involving tunneling nanotubes. FASEB J. **29**, 4695-4712

694   35   Schiller, C., Huber, J. E., Diakopoulos, K. N. and Weiss, E. H. (2013) Tunneling nanotubes
695   enable intercellular transfer of MHC class I molecules. Hum Immunol. **74**, 412-416

696   36   Lou, E., Fujisawa, S., Morozov, A., Barlas, A., Romin, Y., Dogan, Y., Gholami, S., Moreira,
697   A. L., Manova-Todorova, K. and Moore, M. A. (2012) Tunneling nanotubes provide a unique
698   conduit for intercellular transfer of cellular contents in human malignant pleural mesothelioma.
699   PLoS One. **7**, e33093

700   37   Hase, K., Kimura, S., Takatsu, H., Ohmae, M., Kawano, S., Kitamura, H., Ito, M., Watarai,
701   H., Hazelett, C. C., Yeaman, C. and Ohno, H. (2009) M-Sec promotes membrane nanotube
702   formation by interacting with Ral and the exocyst complex. Nat Cell Biol. **11**, 1427-1432

703   38   Gerdes, H. H., Bukoreshtliev, N. V. and Barroso, J. F. (2007) Tunneling nanotubes: a new
704   route for the exchange of components between animal cells. FEBS Lett. **581**, 2194-2201

705   39   Wang, X. and Gerdes, H. H. (2015) Transfer of mitochondria via tunneling nanotubes
706   rescues apoptotic PC12 cells. Cell Death Differ. **22**, 1181-1191

707   40   Sharma, M. and Subramaniam, S. (2019) Rhes travels from cell to cell and transports
708   Huntington disease protein via TNT-like protrusion. J Cell Biol. **218**, 1972-1993

709   41   Chapple, C. E., Robisson, B., Spinelli, L., Guien, C., Becker, E. and Brun, C. (2015) Extreme
710   multifunctional proteins identified from a human protein interaction network. Nat Commun. **6**,
711   7412

712   42   Issaeva, N. (2019) p53 Signaling in Cancers. Cancers (Basel). **11**

713   43   Santucci, R., Sinibaldi, F., Cozza, P., Polticelli, F. and Fiorucci, L. (2019) Cytochrome c: An
714   extreme multifunctional protein with a key role in cell fate. Int J Biol Macromol. **136**, 1237-1246

715   44   Subramaniam, S., Mealer, R. G., Sixt, K. M., Barrow, R. K., Usiello, A. and Snyder, S. H.
716   (2010) Rhes, a physiologic regulator of sumoylation, enhances cross-sumoylation between the
717   basic sumoylation enzymes E1 and Ubc9. J Biol Chem. **285**, 20428-20432

718   45   Rabellino, A., Andreani, C. and Scaglioni, P. P. (2017) The Role of PIAS SUMO E3-Ligases
719   in Cancer. Cancer Res. **77**, 1542-1547

720   46   McManus, F. P., Bourdeau, V., Acevedo, M., Lopes-Paciencia, S., Mignacca, L.,
721   Lamoliatte, F., Rojas Pino, J. W., Ferbeyre, G. and Thibault, P. (2018) Quantitative SUMO
722   proteomics reveals the modulation of several PML nuclear body associated proteins and an
723   anti-senescence function of UBC9. Sci Rep. **8**, 7754

724   47   McManus, F. P., Lamoliatte, F. and Thibault, P. (2017) Identification of cross talk
725   between SUMOylation and ubiquitylation using a sequential peptide immunopurification
726   approach. Nat Protoc. **12**, 2342-2358

727   48   Jia, Y., Claessens, L. A., Vertegaal, A. C. O. and Ovaa, H. (2019) Chemical Tools and
728   Biochemical Assays for SUMO Specific Proteases (SENPs). ACS Chem Biol. **14**, 2389-2395

729   49   Nguyen H.B., Q. L. A. (2012) Encyclopedia of Signaling Molecules. Springer, New York, NY

730   50   Caron, E. (2003) Cellular functions of the Rap1 GTP-binding protein: a pattern emerges. J
731   Cell Sci. **116**, 435-440

732   51   Geiss-Friedlander, R. and Melchior, F. (2007) Concepts in sumoylation: a decade on. Nat
733   Rev Mol Cell Biol. **8**, 947-956

52   Matsuzaki, S., Lee, L., Knock, E., Srikumar, T., Sakurai, M., Hazrati, L. N., Katayama, T., Staniszewski, A., Raught, B., Arancio, O. and Fraser, P. E. (2015) SUMO1 Affects Synaptic Function, Spine Density and Memory. Sci Rep. **5**, 10730

53   Quach, D. H., Oliveira-Fernandes, M., Gruner, K. A. and Tourtellotte, W. G. (2013) A sympathetic neuron autonomous role for Egr3-mediated gene regulation in dendrite morphogenesis and target tissue innervation. J Neurosci. **33**, 4570-4583

54   Kuwajima, T., Nishimura, I. and Yoshikawa, K. (2006) Necdin promotes GABAergic neuron differentiation in cooperation with Dlx homeodomain proteins. J Neurosci. **26**, 5383-5392

55   Heikamp, E. B., Patel, C. H., Collins, S., Waickman, A., Oh, M. H., Sun, I. H., Illei, P., Sharma, A., Naray-Fejes-Toth, A., Fejes-Toth, G., Misra-Sen, J., Horton, M. R. and Powell, J. D. (2014) The AGC kinase SGK1 regulates TH1 and TH2 differentiation downstream of the mTORC2 complex. Nat Immunol. **15**, 457-464

56   Lejard, V., Blais, F., Guerquin, M. J., Bonnet, A., Bonnin, M. A., Havis, E., Malbouyres, M., Bidaud, C. B., Maro, G., Gilardi-Hebenstreit, P., Rossert, J., Ruggiero, F. and Duprez, D. (2011) EGR1 and EGR2 involvement in vertebrate tendon differentiation. J Biol Chem. **286**, 5855-5867

57   Yamauchi, K., Yamazaki, M., Abe, M., Sakimura, K., Lickert, H., Kawasaki, T., Murakami, F. and Hirata, T. (2017) Netrin-1 Derived from the Ventricular Zone, but not the Floor Plate, Directs Hindbrain Commissural Axons to the Ventral Midline. Sci Rep. **7**, 11992

58   Fantin, A., Maden, C. H. and Ruhrberg, C. (2009) Neuropilin ligands in vascular and neuronal patterning. Biochem Soc Trans. **37**, 1228-1232

59   Das, G., Yu, Q., Hui, R., Reuhl, K., Gale, N. W. and Zhou, R. (2016) EphA5 and EphA6: regulation of neuronal and spine morphology. Cell Biosci. **6**, 48

60   Dennis, D. J., Han, S. and Schuurmans, C. (2019) bHLH transcription factors in neural development, disease, and reprogramming. Brain Res. **1705**, 48-65

61   Li, H., Radford, J. C., Ragusa, M. J., Shea, K. L., McKercher, S. R., Zaremba, J. D., Soussou, W., Nie, Z., Kang, Y. J., Nakanishi, N., Okamoto, S., Roberts, A. J., Schwarz, J. J. and Lipton, S. A. (2008) Transcription factor MEF2C influences neural stem/progenitor cell differentiation and maturation in vivo. Proc Natl Acad Sci U S A. **105**, 9397-9402

62   Ozdinler, P. H. and Erzurumlu, R. S. (2002) Slit2, a branching-arborization factor for sensory axons in the Mammalian CNS. J Neurosci. **22**, 4540-4549

63   Sun, L., Li, H., Chen, J., Iwasaki, Y., Kubota, T., Matsuoka, M., Shen, A., Chen, Q. and Xu, Y. (2013) PIASy mediates hypoxia-induced SIRT1 transcriptional repression and epithelial-to-mesenchymal transition in ovarian cancer cells. J Cell Sci. **126**, 3939-3947

64   Yan, C., Yu, C., Zhang, D., Cui, Y., Zhou, J. and Cui, S. (2016) Protein Inhibitor of Activated STAT Y (PIASy) Regulates Insulin Secretion by Interacting with LIM Homeodomain Transcription Factor Isl1. Sci Rep. **6**, 39308

65   Chowdhury, B., Porter, E. G., Stewart, J. C., Ferreira, C. R., Schipma, M. J. and Dykhuizen, E. C. (2016) PBRM1 Regulates the Expression of Genes Involved in Metabolism and Cell Adhesion in Renal Clear Cell Carcinoma. PLoS One. **11**, e0153718

66   West, K. O., Scott, H. M., Torres-Odio, S., West, A. P., Patrick, K. L. and Watson, R. O. (2019) The Splicing Factor hnRNP M Is a Critical Regulator of Innate Immune Gene Expression in Macrophages. Cell Rep. **29**, 1594-1609 e1595

777 67   Zupkovitz, G., Tischler, J., Posch, M., Sadzak, I., Ramsauer, K., Egger, G., Grausenburger,
778 R., Schweifer, N., Chiocca, S., Decker, T. and Seiser, C. (2006) Negative and positive regulation of
779 gene expression by mouse histone deacetylase 1. Mol Cell Biol. **26**, 7913-7928

780 68   Greer, C. B., Tanaka, Y., Kim, Y. J., Xie, P., Zhang, M. Q., Park, I. H. and Kim, T. H. (2015)
781 Histone Deacetylases Positively Regulate Transcription through the Elongation Machinery. Cell
782 Rep. **13**, 1444-1455

783 69   Sharma, M., Jarquin, U. N. R., Rivera, O., Kazantzis, M., Eshraghi, M., Shahani, N.,
784 Sharma, V., Tapia, R. and Subramaniam, S. (2019) Rhes, a striatal-enriched protein, promotes
785 mitophagy via Nix. Proc Natl Acad Sci U S A. **116**, 23760-23771

786 70   Spano, D., Branchi, I., Rosica, A., Pirro, M. T., Riccio, A., Mithbaokar, P., Affuso, A., Arra,
787 C., Campolongo, P., Terracciano, D., Macchia, V., Bernal, J., Alleva, E. and Di Lauro, R. (2004)
788 Rhes is involved in striatal function. Mol Cell Biol. **24**, 5788-5796

789 71   Hickey, C. M., Wilson, N. R. and Hochstrasser, M. (2012) Function and regulation of
790 SUMO proteases. Nat Rev Mol Cell Biol. **13**, 755-766

791 72   Hecker, C. M., Rabiller, M., Haglund, K., Bayer, P. and Dikic, I. (2006) Specification of
792 SUMO1- and SUMO2-interacting motifs. J Biol Chem. **281**, 16117-16127

793 73   Kumar, R., Gonzalez-Prieto, R., Xiao, Z., Verlaan-de Vries, M. and Vertegaal, A. C. O.
794 (2017) The STUbL RNF4 regulates protein group SUMOylation by targeting the SUMO
795 conjugation machinery. Nat Commun. **8**, 1809

796 74   Hendriks, I. A., D'Souza, R. C., Yang, B., Verlaan-de Vries, M., Mann, M. and Vertegaal, A.
797 C. (2014) Uncovering global SUMOylation signaling networks in a site-specific manner. Nat
798 Struct Mol Biol. **21**, 927-936

799 75   Ciobanu, D. C., Lu, L., Mozhui, K., Wang, X., Jagalur, M., Morris, J. A., Taylor, W. L., Dietz,
800 K., Simon, P. and Williams, R. W. (2010) Detection, validation, and downstream analysis of
801 allelic variation in gene expression. Genetics. **184**, 119-128

802 76   Liu, H. W., Zhang, J., Heine, G. F., Arora, M., Gulcin Ozer, H., Onti-Srinivasan, R., Huang,
803 K. and Parvin, J. D. (2012) Chromatin modification by SUMO-1 stimulates the promoters of
804 translation machinery genes. Nucleic Acids Res. **40**, 10172-10186

805 77   Rosonina, E., Akhter, A., Dou, Y., Babu, J. and Sri Theivakadadcham, V. S. (2017)
806 Regulation of transcription factors by sumoylation. Transcription. **8**, 220-231

807 78   David, G., Neptune, M. A. and DePinho, R. A. (2002) SUMO-1 modification of histone
808 deacetylase 1 (HDAC1) modulates its biological activities. J Biol Chem. **277**, 23658-23663

809 79   Joung, H., Kwon, S., Kim, K. H., Lee, Y. G., Shin, S., Kwon, D. H., Lee, Y. U., Kook, T., Choe,
810 N., Kim, J. C., Kim, Y. K., Eom, G. H. and Kook, H. (2018) Sumoylation of histone deacetylase 1
811 regulates MyoD signaling during myogenesis. Exp Mol Med. **50**, e427

812 80   Tao, C. C., Hsu, W. L., Ma, Y. L., Cheng, S. J. and Lee, E. H. (2017) Epigenetic regulation of
813 HDAC1 SUMOylation as an endogenous neuroprotection against Abeta toxicity in a mouse
814 model of Alzheimer's disease. Cell Death Differ. **24**, 597-614

815 81   Nathan, D., Ingvarsdottir, K., Sterner, D. E., Bylebyl, G. R., Dokmanovic, M., Dorsey, J. A.,
816 Whelan, K. A., Krsmanovic, M., Lane, W. S., Meluh, P. B., Johnson, E. S. and Berger, S. L. (2006)
817 Histone sumoylation is a negative regulator in Saccharomyces cerevisiae and shows dynamic
818 interplay with positive-acting histone modifications. Genes Dev. **20**, 966-976

819   82   Zhang, R., Mehla, R. and Chauhan, A. (2010) Perturbation of host nuclear membrane
820   component RanBP2 impairs the nuclear import of human immunodeficiency virus -1
821   preintegration complex (DNA). PLoS One. **5**, e15620
822   83   Turpin, P., Ossareh-Nazari, B. and Dargemont, C. (1999) Nuclear transport and
823   transcriptional regulation. FEBS Lett. **452**, 82-86
824   84   Vassileva, M. T. and Matunis, M. J. (2004) SUMO modification of heterogeneous nuclear
825   ribonucleoproteins. Mol Cell Biol. **24**, 3623-3632
826   85   Kirsh, O., Seeler, J. S., Pichler, A., Gast, A., Muller, S., Miska, E., Mathieu, M., Harel-
827   Bellan, A., Kouzarides, T., Melchior, F. and Dejean, A. (2002) The SUMO E3 ligase RanBP2
828   promotes modification of the HDAC4 deacetylase. EMBO J. **21**, 2682-2691
829   86   Pozzi, B., Bragado, L., Will, C. L., Mammi, P., Risso, G., Urlaub, H., Luhrmann, R. and
830   Srebrow, A. (2017) SUMO conjugation to spliceosomal proteins is required for efficient pre-
831   mRNA splicing. Nucleic Acids Res. **45**, 6729-6745
832   87   Laplante, M. and Sabatini, D. M. (2013) Regulation of mTORC1 and its impact on gene
833   expression at a glance. J Cell Sci. **126**, 1713-1719
834   88   Kunkel, J., Luo, X. and Capaldi, A. P. (2019) Integrated TORC1 and PKA signaling control
835   the temporal activation of glucose-induced gene expression in yeast. Nat Commun. **10**, 3558
836   89   Yapo, C., Nair, A. G., Hellgren Kotaleski, J., Vincent, P. and Castro, L. R. V. (2018) Switch-
837   like PKA responses in the nucleus of striatal neurons. J Cell Sci. **131**
838   90   Galisson, F., Mahrouche, L., Courcelles, M., Bonneil, E., Meloche, S., Chelbi-Alix, M. K.
839   and Thibault, P. (2011) A novel proteomics approach to identify SUMOylated proteins and their
840   modification sites in human cells. Mol Cell Proteomics. **10**, M110 004796
841   91   Lamoliatte, F., Bonneil, E., Durette, C., Caron-Lizotte, O., Wildemann, D., Zerweck, J.,
842   Wenshuk, H. and Thibault, P. (2013) Targeted identification of SUMOylation sites in human
843   proteins using affinity enrichment and paralog-specific reporter ions. Mol Cell Proteomics. **12**,
844   2536-2550
845   92   Tammsalu, T., Matic, I., Jaffray, E. G., Ibrahim, A. F., Tatham, M. H. and Hay, R. T. (2015)
846   Proteome-wide identification of SUMO modification sites by mass spectrometry. Nat Protoc.
847   **10**, 1374-1388
848   93   Lamoliatte, F., McManus, F. P., Maarifi, G., Chelbi-Alix, M. K. and Thibault, P. (2017)
849   Uncovering the SUMOylation and ubiquitylation crosstalk in human cells using sequential
850   peptide immunopurification. Nat Commun. **8**, 14109
851   94   Lamoliatte, F., Caron, D., Durette, C., Mahrouche, L., Maroui, M. A., Caron-Lizotte, O.,
852   Bonneil, E., Chelbi-Alix, M. K. and Thibault, P. (2014) Large-scale analysis of lysine SUMOylation
853   by SUMO remnant immunoaffinity profiling. Nat Commun. **5**, 5409
854   95   Li, C., McManus, F. P., Plutoni, C., Pascariu, C. M., Nelson, T., Alberici Delsin, L. E., Emery,
855   G. and Thibault, P. (2020) Quantitative SUMO proteomics identifies PIAS1 substrates involved in
856   cell migration and motility. Nat Commun. **11**, 834
857   96   Eshraghi, M., Karunadharma, P., Blin, J., Shahani, N., Ricci, E., Michel, A., Urban, N., Galli,
858   N., Rao, S. R., Sharma, M., Florescu, K. and Subramaniam, S. (2019) Global ribosome profiling
859   reveals that mutant huntingtin stalls ribosomes and represses protein synthesis independent of
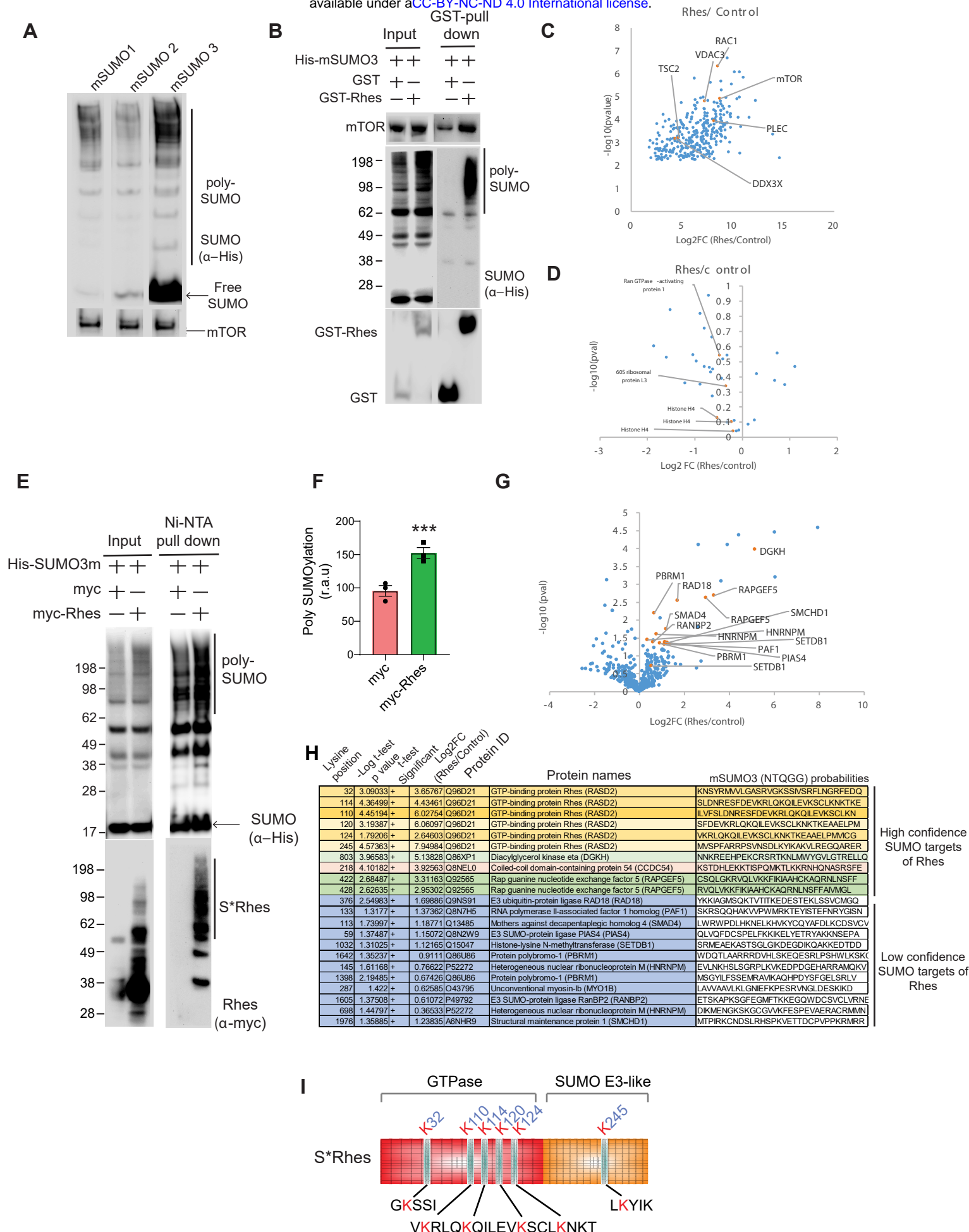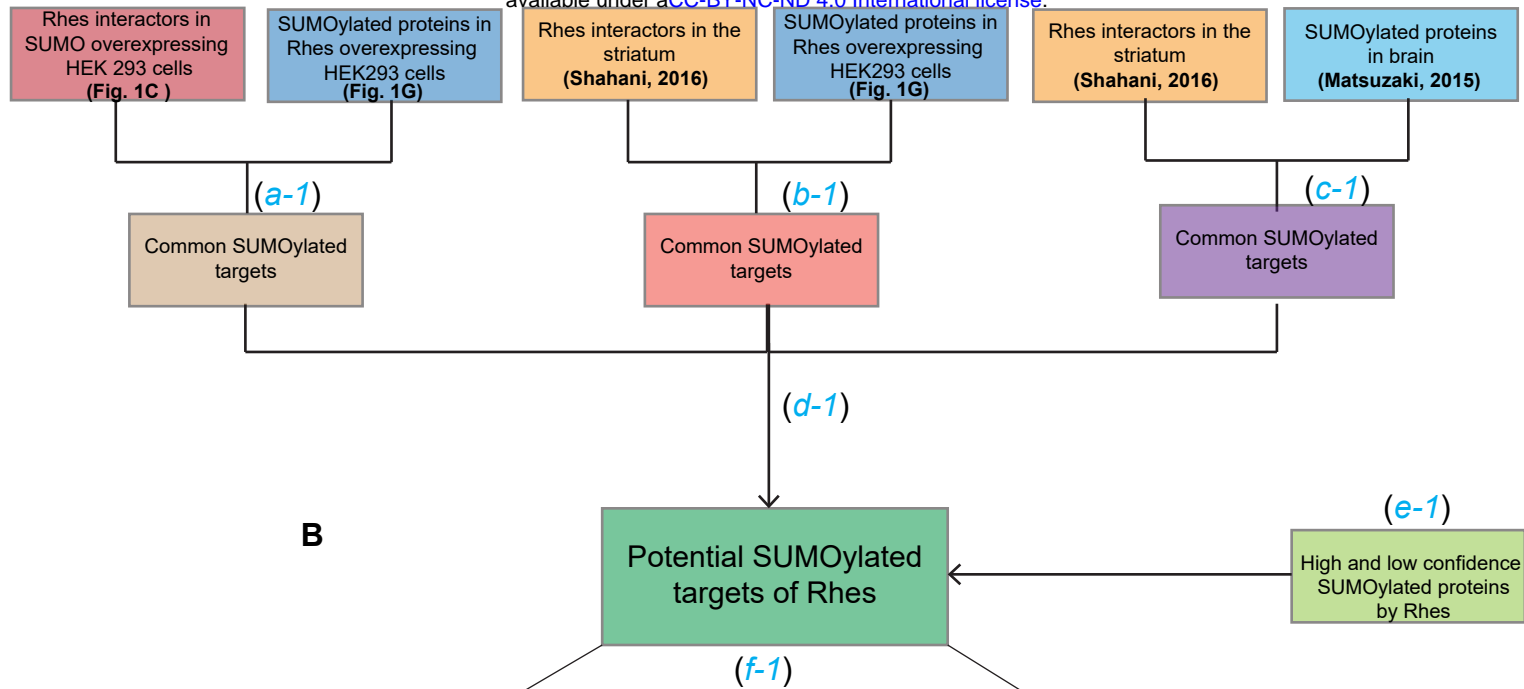860   fragile X mental retardation protein. BioRxiv
861

Figure 1

A

B

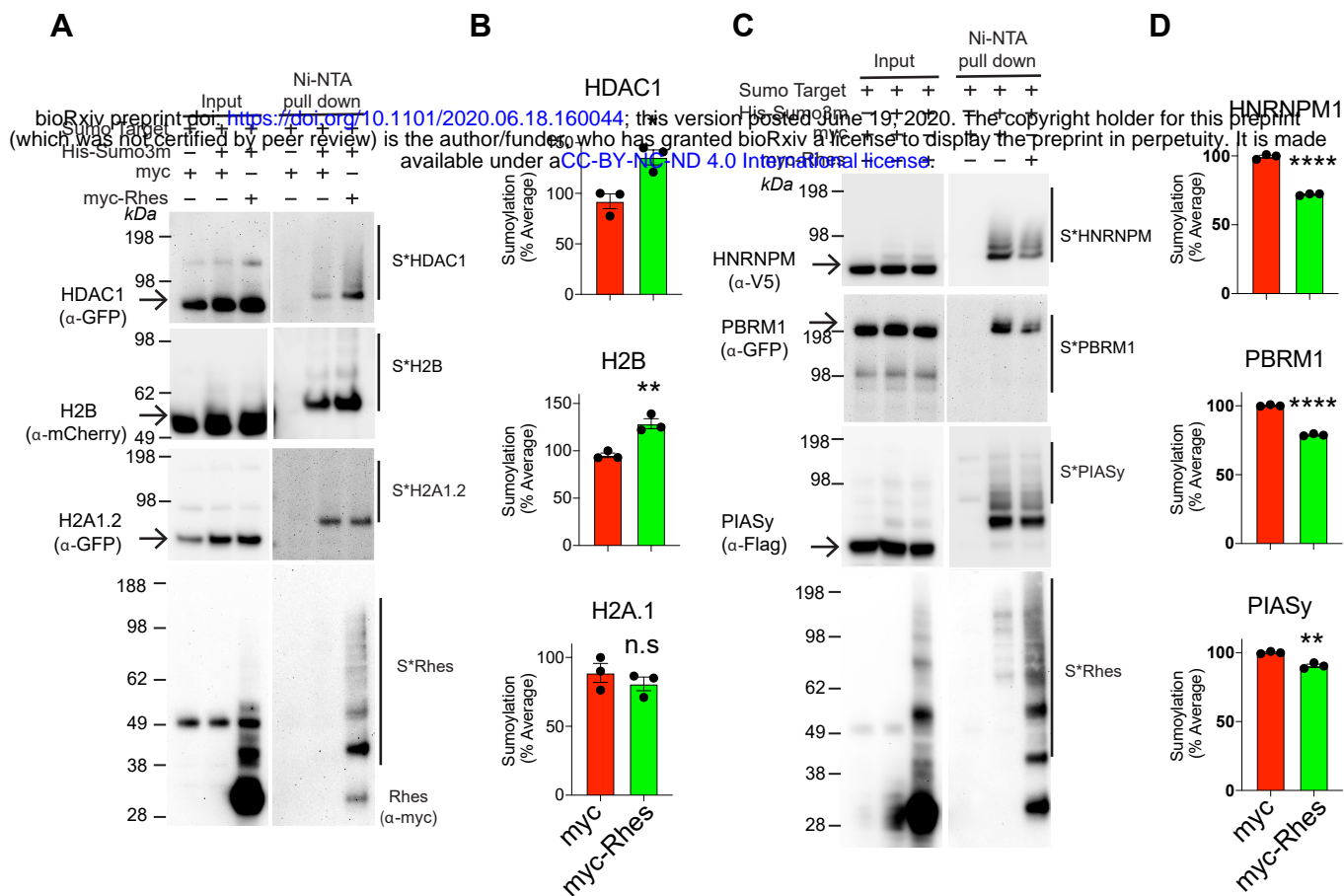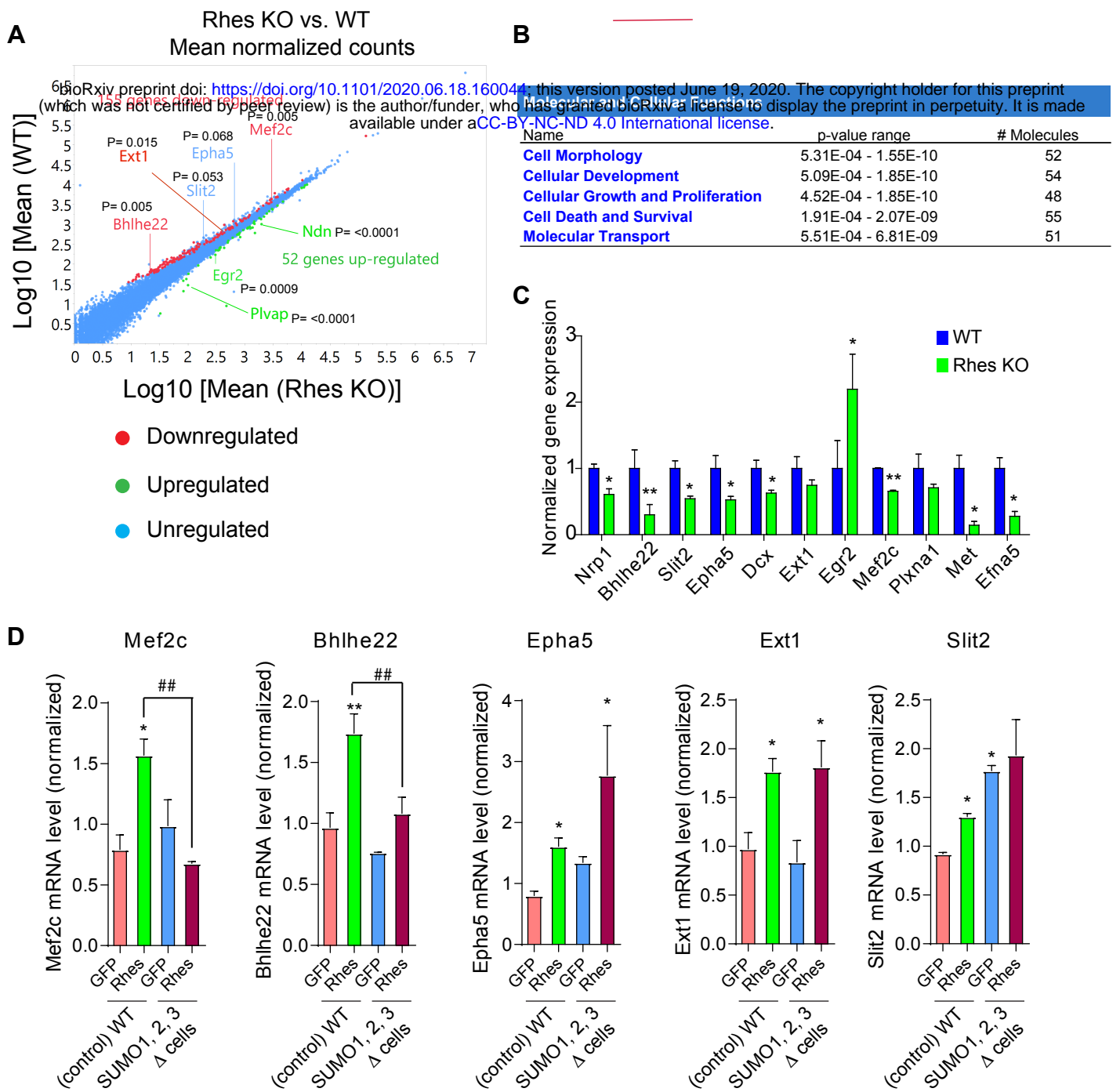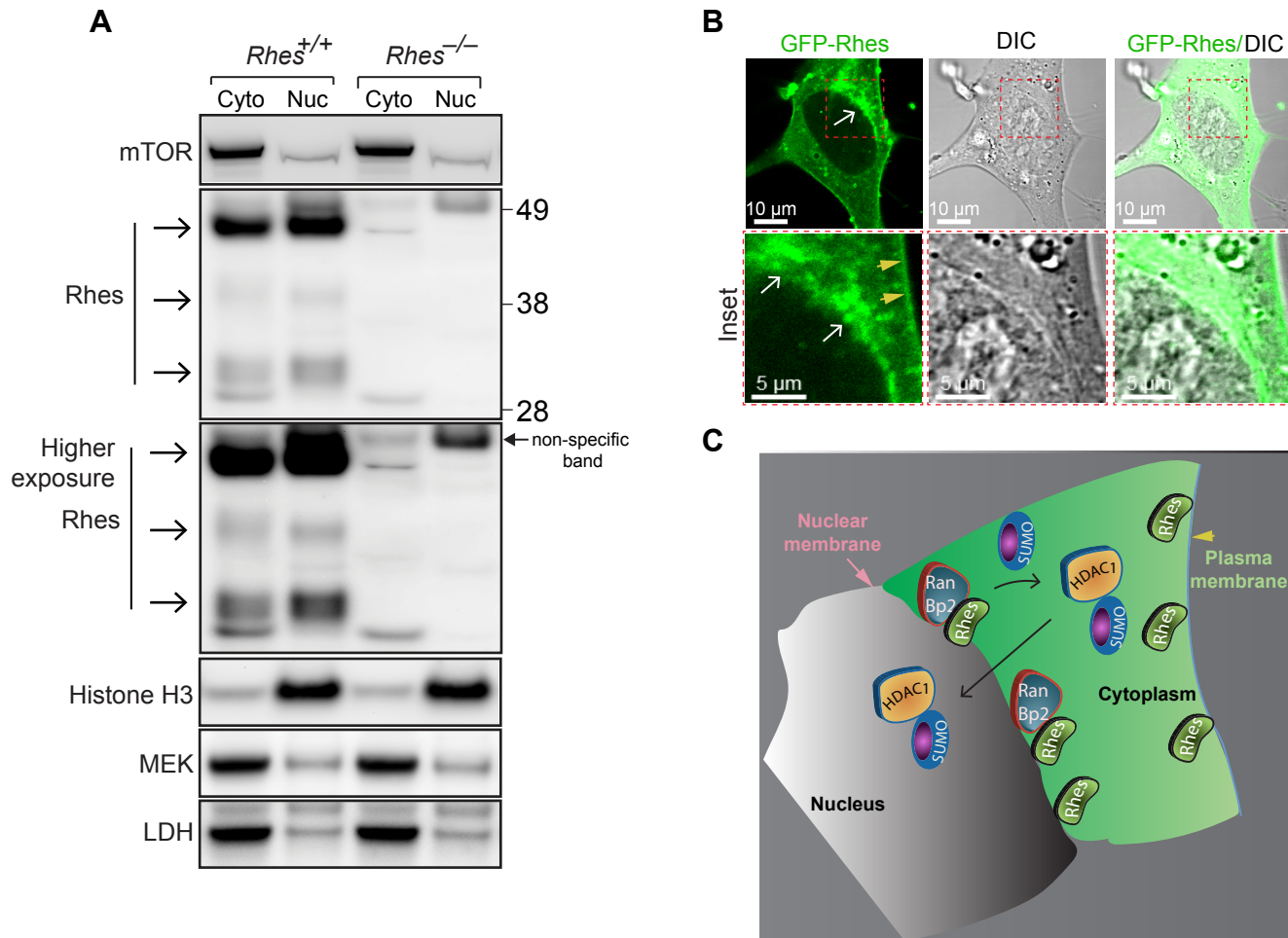| Potential SUMO targets of Rhes	Functions
HDAC1	Histone Deacetylase
PAF1	Paf1/RNA Polymerase II Complex Component
hPIASy	E3 SUMO-Protein Ligase PIAS4
NPM	Nucleophosmin 1
L26	Ribosomal Protein L26
RBBP4	Retinoblastoma-Binding Protein P48
H2B	Histone 2B
Pebb-II-I	TFII-I beta isoform
PCNA	Proliferating Cell Nuclear Antigen
CDK1	Cyclin Dependent Kinase 1
SAFB1	Scaffold Attachment Factor B
MATR3	a nuclear matrix protein
DGK	Diacylglycerol Kinase Beta
DDX3	DEAD-Box Helicase 3
H2A1.2	H2A histone family member Y
Ku70	p70/p80 autoantigen is a nuclear complex
Actin-3	Actin
Vimentin	class-III intermediate filaments
HshnRNPM	heterogeneous nuclear ribonucleoproteins
PBRM1	chromatin-remodeling complexes
Syt1	Synaptotagmin 1
Hrad18	E3 Ubiquitin Protein Ligase
HnRNPC	nuclear ribonucleoproteins
Smad4	transcription factor
NUMA	nuclea matrix
SF3B1	Pre-MRNA Splicing Factor
PRKAR2B	CAMP-Dependent Protein Kinase Type II-Beta

Figure 2

Figure 3

A

Rhes KO vs. WT
Mean normalized counts

B

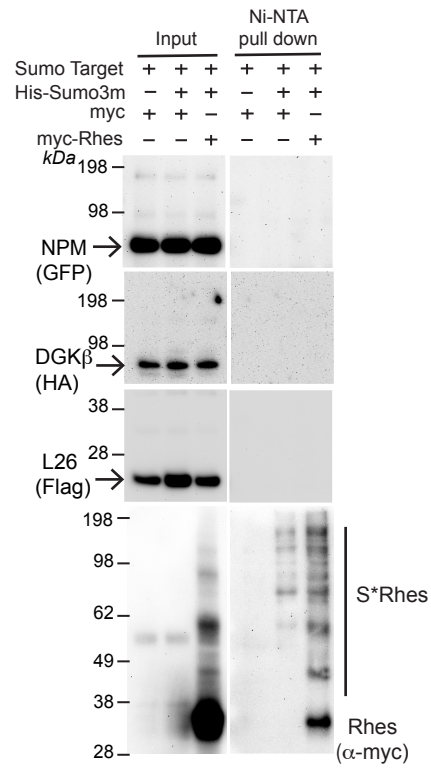| Name	p-value range	# Molecules
Cell Morphology	5.31E-04 - 1.55E-10	52
Cellular Development	5.09E-04 - 1.85E-10	54
Cellular Growth and Proliferation	4.52E-04 - 1.85E-10	48
Cell Death and Survival	1.91E-04 - 2.07E-09	55
Molecular Transport	5.51E-04 - 6.81E-09	51

Figure 4

Figure 5

Supplementary Figure 1